In-resonance decay channel detection

Seokhyeon Song

March 18, 2025

(Introduction here?)

The exact propagator of a scalar field can be written in a form of

$$\Delta(p^2) = \frac{i}{p^2 - M_0^2 + \Pi(p^2)},$$

where the self-energy $\Pi(p^2)$ contains the sum of 1PI loop integrals. Following the "real on-shell" renormalisation convention, the propagator is

$$\Delta(p^2) = \frac{i}{p^2 - M^2 + \Pi(p^2) - \operatorname{Re}\Pi(M^2)} = \frac{iZ}{p^2 - M^2 + iZ\operatorname{Im}\Pi(p^2) + O((p^2 - M^2)^2)},$$

where the real on-shell mass M and the field-strength renormalisation Z satisfy

$$\begin{aligned} M^2 &= M_0^2 - \operatorname{Re}\Pi(M^2), \\ Z^{-1} &= 1 + \operatorname{Re}\left[\frac{d\Pi(p^2)}{d(p^2)}\right]_{p^2 = M^2}. \end{aligned}$$

(Particles near threshold ref. here) The imaginary part of the denominator of the propagator is related to the particle's total decay width Γ, where

$$M\Gamma = Z\operatorname{Im}\Pi(M^2).$$

Because of unitarity, this definition of decay width coincides with the definition given by the scattering amplitude with one initial state. (More rigorous statement needed. Actually only well-defined in NWA?)

One of the alternative definition uses the complex pole mass $\tilde{M}_p$, where the propagator diverges at $p^2 = \tilde{M}_p^2$. In this framework, the real particle mass M_p and the width Γ_p can be read,

$$\tilde{M}_p = M_p - \frac{i}{2}\Gamma_p.$$

This definition seems to be mathematically more concise, but there are subtleties. In terms of complex plane of p^2, the physical Riemann sheet consists of the positive-imaginary half plane and its Schwarz reflection. In this sheet, the propagator has no pole. In order to get a pole, we have to perform analytic continuation across a branch cut starting from $p^2 = M_{\text{th}}^2$, where the "threshold invariant mass" M_{th} is a sum of the masses of decay products. If there are more than one available decay channels, then there can be more than one secondary Riemann sheets, each contains complex pole.

If all the threshold invariant masses are sufficiently out off the resonance peak, we can analytically continue the Riemann sheet through the branch near the peak and obtain the complex pole,

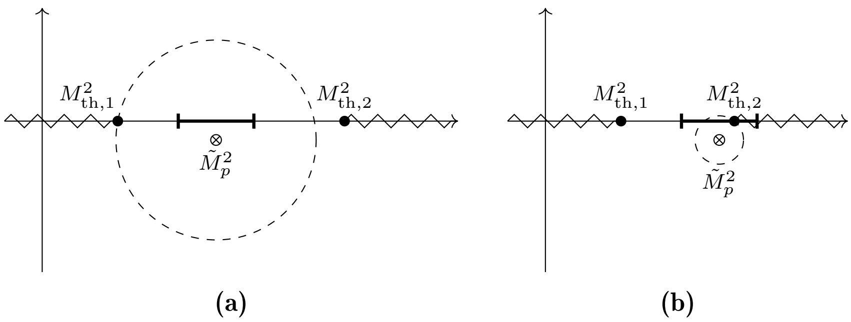

Figure 1: Diagrams demonstrating complex-analytic structure of the propagator $\Delta(p^2)$, drawn on a complex plane of p^2. The thick interval indicates the range of resonance peak, and the Riemann sheet is analytically continued through the midpoint of peak. The small circles with cross displays the position of a pole on a secondary Riemann sheet, and the dashed circles means the radius of convergence of the self-energy function $\Pi(p^2)$, centered on the pole. (a) If every threshold invariant masses are far from the peak, the entirety of peak lies well inside the radius of convergence. Hence, we can take a linear approximation of the self-energy. (b) If there is a threshold invariant mass inside the peak, the self-energy is non-analytic. Thus a linear approximation breaks down.

which agrees well with the real on-shell mass and width. The reason is that because the self energy $\Pi(p^2)$ is an analytic function of p^2 except on the poles and branch singularities, we may linearly approximate

$$p^2 - M_0^2 + \Pi(p^2) \simeq Z_p^{-1}(p^2 - \tilde{M}_p^2)$$

near the peak, where Z_p^{-1} is the residue of propagator on the pole $p^2 = \tilde{M}_p^2$. Then

$$\Delta(p^2) \simeq \frac{iZ_p}{p^2 - \tilde{M}_p^2} = \frac{iZ_p}{p^2 - (M_p^2 - \frac{\Gamma_p^2}{4}) + iM_p\Gamma_p},$$

suggesting Breit-Wigner distribution. The analytic behavior of the propagator also can be seen in Fig. 1. Typically, decay width of a particle is way smaller than a mass, so we can neglect the Γ_p^2 term.

However, if there is an "in-resonance" decay channel whose threshold invariant mass lies inside the peak, then there exists a branch singularity inside the peak on the real axis, hence such linear approximation is invalid. In this case, depending on the point of view, one can say that more than one pole is involving in the resonance, or that no pole explains the resonance well enough. Even in this case, the real on-shell definition serves as a definition of the unique mass and width, therefore, the mass and width from now on will only mean the real on-shell values.

1 Resonance Shape

In the presence of in-resonance decay channel, a shape of resonance peak does not resemble the Breit-Wigner distribution, and a nontrivial momentum dependence of a self-energy becomes important. We will consider one-loop corrections to the scalar particle propagator in terms of renormalisable couplings. The momentum dependent contributions in self-energy come from loop diagrams with 2 three-particle vertices. For example, consider the following real scalar theory:

$$\mathcal{L} = \frac{1}{2}\partial_\mu X \partial^\mu X - \frac{1}{2}M^2X^2 + \mathcal{L}_{\mathrm{int}}.$$

If a particle ϕ which has a mass m interacts with X, a process $X \to \phi\bar{\phi}$ has a threshold invariant mass $M_{\text{th}} = 2m$. Then the self-energy $\Pi(p^2)$ of X has a branch singularity at $p^2 = 4m^2$, but the behaviour of such singularity depends on the spin of ϕ.

If ϕ is a scalar particle, a complex scalar with $\mathcal{L}_{\text{int}} = gX\phi^*\phi$ for this example, the most singular part of $\Pi(p^2)$ near threshold is

$$\Pi(p^2) = (\text{regular}) - \text{sgn}(4m^2 - p^2)\frac{g^2}{32\pi m}\sqrt{4m^2 - p^2} + O((4m^2 - p^2)^{3/2}).$$

As a function of real variable p^2, this means that $\Pi(p^2)$ is continuous but non-differentiable at $p^2 = 4m^2$. This leads to a typical cusp shape in resonance, as shown in Fig. 2a. On the other hand, if ϕ is a spinor with $\mathcal{L}_{\text{int}} = gX\bar{\phi}\phi$, then the most singular part of $\Pi(p^2)$ is

$$\Pi(p^2) = (\text{regular}) + \text{sgn}(4m^2 - p^2)\frac{y^2}{16\pi m}(4m^2 - p^2)^{3/2} + O((4m^2 - p^2)^{5/2}).$$

This means that $\Pi(p^2)$ is differentiable at $p^2 = 4m^2$. This softer singularity suggests that there is no harsh momentum dependence presenting in the resonance shape, as in Fig. 2b. If we only look at the imaginary part of the self-energy in $p^2 > 4m^2$ region, these spin-dependent results can be reinterpreted as being due to the phase space suppression of decay products.

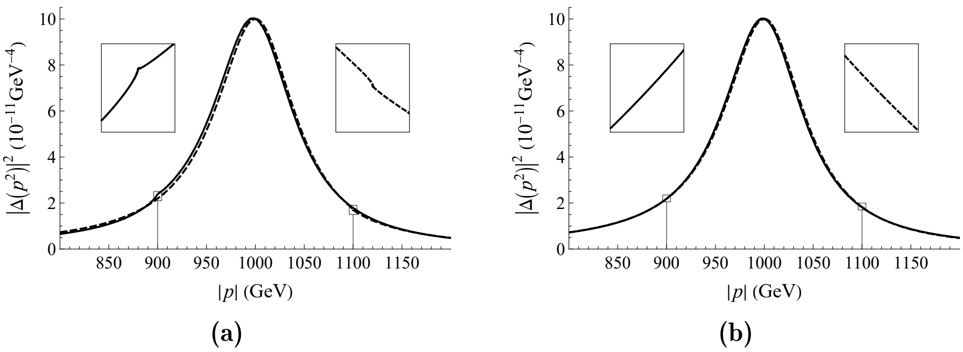

Figure 2: Graphs demonstrating resonance shapes of a real scalar particle X up to one-loop order, when the loop particle is (a) a complex scalar and (b) a Dirac fermion. In both cases, the on-shell mass of X is 1 TeV and the width of X is 100 GeV. For the solid lines, loop particle mass is 450 GeV, so the threshold invariant mass is 900 GeV. The partial width due to the decaying of X into two loop particle is 50 GeV, and the remaining 50 GeV width is assumed to be due to decay into light particles. For the dashed lines, loop particle mass is 550 GeV, so the threshold invariant mass is 1100 GeV. Here the loop particles do not contribute to the on-shell decay, so all of the width is coming from the light particles. Supplementary graphs show the resonance shapes near the threshold invariant mass.

2 Toy Statistical Analysis

One of standard statistical tests for discovering new physics model is the likelihood-ratio test. Suppose that a collection S of physical observables follows the probability distribution $\rho(S;\theta)$ under a set of model parameters θ. For example, in collider experiments, S may contain the type and momentum of final-state particles. If we perform N successive experiments, the log-likelihood of a particular collection of parameter values θ is defined as

$$L(\theta) = \sum_{i=1}^{N} \ln \rho(S_i;\theta).$$

In most cases, the null hypothesis constrains the parameter space to a certain subset Θ_0. On the other hand, the alternative hypothesis includes the entire parameter space Θ. For each hypothesis, the best fit is given by maximising the log-likelihood function. In a likelihood-ratio test, the test statistic is a difference of maximised log-likelihood function in both parameter space, that is,

$$t := 2\left[\max_{\theta\in\Theta} L(\theta) - \max_{\theta\in\Theta_0} L(\theta)\right].$$

The test statistic t follows some probability distribution, for example, Wilks' theorem shows that t follows a χ^2 distribution under certain assumptions.

In this paper, we will discuss toy statistical analysis under some simplifying assumptions. These assumptions may not hold in real experiment, but statistical analysis of a real experiment requires a lot of information about experimental settings and a detail of new physics model. In any case, this simple analysis can be thought of as an approximate analysis of the observability of in-resonance effects. We will focus on the dimuon production in accelerators, and ignore other final-state particles. We also ignore the angular dependence and only focus on invariant mass μ of dimuon.

We divide the total probability distribution $\rho(\mu)$ of dimuon invariant mass into three parts; $\rho_0(\mu)$ is the SM "background", $\rho_1(\mu)$ is the Breit-Wigner best fit of the resonance signal, and $\rho_2(\mu)$ is the rest. Note that both ρ_0 and ρ_1 should be positive but ρ_2 can be negative. These three distributions correspond to three different hypotheses, suggesting different physical conclusions:

$H_0 : \rho = \rho_0;$ There is only SM background (no scalar resonance discovered),

$H_1 : \rho = \rho_0 + \rho_1;$ There is scalar resonance, but it is Breit-Wigner (no in-resonance channel detected),

$H_2 : \rho = \rho_0 + \rho_1 + \rho_2;$ There is scalar resonance with in-resonance channel.

Furthermore, we also assume that the background is very large relative to the signal and does not change significantly within the mass range $M - \Delta M \le \mu \le M + \Delta M$ that we are interested in:

$$\rho_0(\mu) \simeq \langle\rho\rangle \gg \rho_1(\mu) > \rho_2(\mu).$$

Each dimuon production signal with invariant mass μ_i contributes to the log-likelihood function by $\ln \rho(\mu_i)$, so

$$L = \sum_{i=1}^{N} \ln \rho(\mu_i).$$

When N is large enough, the sum can be interpreted as a Monte Carlo integral. Here the distribution is almost uniform within the mass range, so

$$L \simeq \frac{N}{2\Delta M}\int_{M-\Delta M}^{M+\Delta M} \ln \rho(\mu)\, d\mu.$$

For two similar distributions $\rho(\mu)$ and $\rho'(\mu) = \rho(\mu) + \Delta\rho(\mu)$, expanding the logarithm gives

$$\ln \rho'(\mu) \simeq \ln \rho(\mu) + \frac{\rho'(\mu) - \rho(\mu)}{\rho(\mu)} - \frac{[\rho'(\mu) - \rho(\mu)]^2}{2\rho(\mu)^2}.$$

Hence,

$$L' - L \simeq \frac{N}{2\Delta M}\int_{M-\Delta M}^{M+\Delta M} \frac{\rho'(\mu) - \rho(\mu)}{\rho(\mu)}\, d\mu - \frac{N}{4\Delta M}\int_{M-\Delta M}^{M+\Delta M} \frac{[\rho'(\mu) - \rho(\mu)]^2}{\rho(\mu)^2}\, d\mu.$$

The first integral is usually zero since ρ and ρ' are both best-fit distributions (thus matching mean values), so

$$L' - L \simeq$$

Then the total log-likelihood is

$$L \simeq \sum_{i=1}^{N} \left(\ln\langle\rho\rangle + \frac{\rho(\mu_i) - \langle\rho\rangle}{\langle\rho\rangle} - \frac{[\rho(\mu_i) - \langle\rho\rangle]^2}{2\langle\rho\rangle^2} \right).$$

When N is large enough, the sum can be interpreted as a Monte Carlo integral. Here the distribution is almost uniform within the mass range, so

$$\begin{aligned}
L &\simeq \frac{N}{2\Delta M} \int_{M-\Delta M}^{M+\Delta M} \left(\ln\langle\rho\rangle + \frac{\rho(\mu_i) - \langle\rho\rangle}{\langle\rho\rangle} - \frac{[\rho(\mu_i) - \langle\rho\rangle]^2}{2\langle\rho\rangle^2} \right) d\mu \\
&= N \ln\langle\rho\rangle + \frac{N}{2\Delta M\langle\rho\rangle} \int_{M-\Delta M}^{M+\Delta M} [\rho(\mu) - \langle\rho\rangle]\, d\mu - \frac{N}{4\Delta M\langle\rho\rangle^2} \int_{M-\Delta M}^{M+\Delta M} [\rho(\mu_i) - \langle\rho\rangle]^2\, d\mu \\
&= N \ln\langle\rho\rangle - \frac{N}{4\Delta M\langle\rho\rangle^2} \int_{M-\Delta M}^{M+\Delta M} [\rho(\mu_i) - \langle\rho\rangle]^2\, d\mu.
\end{aligned}$$

Therefore,

$$t_1 := 2L(H_1) - 2L(H_0) = \frac{N}{4\Delta M\langle\rho\rangle^2} \int_{M-\Delta M}^{M+\Delta M} [\rho(\mu_i) - \langle\rho\rangle]^2\, d\mu.$$